

# Collective Motion and Phase Transitions of Symmetric Camphor Boats

Eric Heisler,<sup>1</sup> Nobuhiko J. Suematsu,<sup>2,3</sup> Akinori Awazu,<sup>1</sup> and Hiraku Nishimori<sup>1</sup>

<sup>1</sup>*Department of Mathematical and Life Sciences, Hiroshima University,  
1-3-1 Kagamiyama, Higashi-Hiroshima 739-8526, Japan*

<sup>2</sup>*Graduate School of Advanced Mathematical Sciences, Meiji University,  
1-1-1 Higashimita, Tamaku, Kawasaki 214-8571, Japan*

<sup>3</sup>*Meiji Institute for Advanced Study of Mathematical Sciences (MIMS),  
1-1-1 Higashimita, Tamaku, Kawasaki 214-8571, Japan*

(Dated: February 8, 2019)

A model describing the motion of several symmetric camphor boats in one dimension displays spontaneous pattern formation and kinetic phase transitions. By varying the viscous resistance in the system, it is possible to form a stationary state, oscillations, or unidirectional flow. In addition, there are qualitatively different dynamical patterns ranging from highly ordered formations to erratic oscillations. Here, we describe and analyze the properties of these behaviors and their transitions.

PACS numbers: 64.60.cn, 05.65.+b, 45.50.-j

The collective motion of many simple elements is a topic with a broad range of applications, from understanding biological group behavior [1–3] to modeling mechanical systems [4, 5]. Accordingly, there have been numerous studies on simplified mathematical models of collective motion. Of particular relevance to this paper is the class of Self Propelled Particles (SPPs) as described by Vicsek *et al.* [6]. Although the original, rule-based SPP models are very simple, they have displayed a variety of complex behaviors including kinetic phase transitions [6–9] and large scale pattern formation [10]. Some extensions of this idea have been made to describe more specific, physically realistic systems [11–14]. These variations often display self organization similar to the more basic models. The benefit of these more specific models is their application to real systems.

The model presented in this paper is further removed from the minimal SPP model than most other variations, but shares some of the basic features, and displays pattern formation and phase transitions similar to those of SPPs. This model describes the motion of an ensemble of symmetric camphor boats (CBs) moving in one dimension. Ensembles of asymmetric CBs have been studied experimentally [15, 16], but are different in that they have a fixed orientation and are driven in a specified direction. Two dimensional experiments with symmetric camphor particles have displayed spontaneous pattern formation, which was attributed to hydrodynamic interactions [17]. Though this phenomenon may be related to the results presented here, our model ignores all hydrodynamic interactions and the boats being modeled are fundamentally different from camphor particles. The reason for using this more complicated and specific model is the potential for experimental verification. It may be difficult or impossible to control relevant parameters in many systems that are described by SPPs, such as flocks of birds or schools of fish, but CB systems are relatively compact and controllable. In the future we hope to experimentally

test the results presented here.

There are three major differences between this model and basic SPP models. SPPs are particles that always move at a constant speed. In our CB model, as well as many previously mentioned variations [11–14], boats are subject to acceleration arising from various forces. However, there is an equilibrium speed corresponding to that of a free flowing boat. Also, The direction of travel of SPPs is instantaneously set depending on neighboring particles. CBs are influenced by collisions with other boats and by a surface tension gradient. The latter being determined by all nearby boats as well as the time history of that region. One more very crucial difference is that there is no noise intentionally added to this system. Most other SPP models depend on added noise, and some use it as a key parameter.

In numerical simulations of the CB model, we observed two distinct kinetic phase transitions by varying the viscous resistance. One appears as the abrupt formation of a stationary, ordered pattern, and the other as a discontinuity in the mean velocity  $|\langle v \rangle|$  of the entire system. Aside from these transitions, a variety of collective behaviors were observed such as synchronized formations and erratic oscillations. Here we will describe some of these behaviors and present quantitative evidence for the phase transitions and pattern formation.

The model being considered describes the motion of thin plastic disks which float on the surface of water. Smaller, circular camphor pellets are attached to the center of the underside of the disks. As the camphor dissolves and diffuses in the water, it changes the surface tension and thus provides a driving force for the plastic disks. These camphor boats are similar to those described in [18], but the boats used here are constructed symmetrically, so there is no preferential direction of travel. The boats move in a circular channel with circumference  $R$ , which is narrow enough to restrict the motion to one dimension. The 1-D equations of motion

are given by (1).

$$\frac{\partial^2 x}{\partial t^2} = -\frac{\mu}{m} \frac{\partial x}{\partial t} + \frac{L}{m} [\gamma(c(x+L/2)) - \gamma(c(x-L/2))] \quad (1)$$

where  $m$  is the mass of the boat,  $\mu$  is the viscosity constant of the water and  $L$  is the diameter of the boat. The position,  $x$ , representing the center of the boat, is defined on a periodic domain with period  $R$ . The second term on the right represents the difference in surface tension between the front and back of the boat as a function of the camphor concentration given by  $c(x+L/2)$  and  $c(x-L/2)$  respectively.  $\gamma(c)$  is approximated by the sigmoidal function in eq.2.

$$\gamma(c) = \frac{\gamma_{water} - \gamma_{camphor}}{(\beta c)^2 + 1} + \gamma_{camphor} \quad (2)$$

$\gamma_{water}$  and  $\gamma_{camphor}$  are the surface tension of pure water and camphor saturated solution respectively.

The concentration of camphor molecules on the surface of the water is constantly changing due to several processes. For a system with  $N$  boats, it can be approximated by the following reaction-diffusion equation (3).

$$\frac{\partial c}{\partial t} = D \frac{\partial^2 c}{\partial x^2} - kc + \alpha \sum_{i=1}^N F(x - x_i) \quad (3)$$

$$F(x) = 1 : \text{for } |x| \leq r_0, \quad 0 : \text{otherwise}$$

Here,  $D$  is the diffusion constant,  $k$  is a constant combining the effects of evaporation and dissolution, and  $\alpha F(x - x_i)$  represents the addition of camphor by each boat's pellet, which is centered at the point  $x_i$  and has radius  $r_0$ . To non-dimensionalize the problem, we define the following dimensionless quantities.

$$t' = t \frac{D}{L^2}, \quad x' = \frac{x}{L}, \quad c' = c\beta \quad (4)$$

Then the dimensionless parameters of the system become

$$\mu' = \frac{\mu L^2}{mD}, \quad k' = \frac{kL^2}{D}, \quad \Gamma = \frac{L^3(\gamma_w - \gamma_c)}{mD^2} \quad (5)$$

$$r'_0 = \frac{r_0}{L}, \quad R' = \frac{R}{L}, \quad \alpha' = \frac{\alpha\beta L^2}{D}$$

Dropping the ' marks, the non-dimensional equations are

$$\frac{\partial^2 x_i}{\partial t^2} = -\mu \frac{\partial x_i}{\partial t} + \Gamma \left[ \frac{1}{c(x_i + \frac{1}{2})^2 + 1} - \frac{1}{c(x_i - \frac{1}{2})^2 + 1} \right]$$

$$\frac{\partial c}{\partial t} = \frac{\partial^2 c}{\partial x^2} - kc + \alpha \sum_{i=1}^N F(x - x_i) \quad (6)$$

$$F(x) = 1 : \text{for } |x| < r_0, \quad 0 : \text{otherwise}$$

In numerical simulations, three distinct categories of behavior were observed. Listed in order of decreasing viscosity, these are: **(I)**stationary equilibrium, **(II)**oscillation, **(III)**unidirectional flow. Examples of

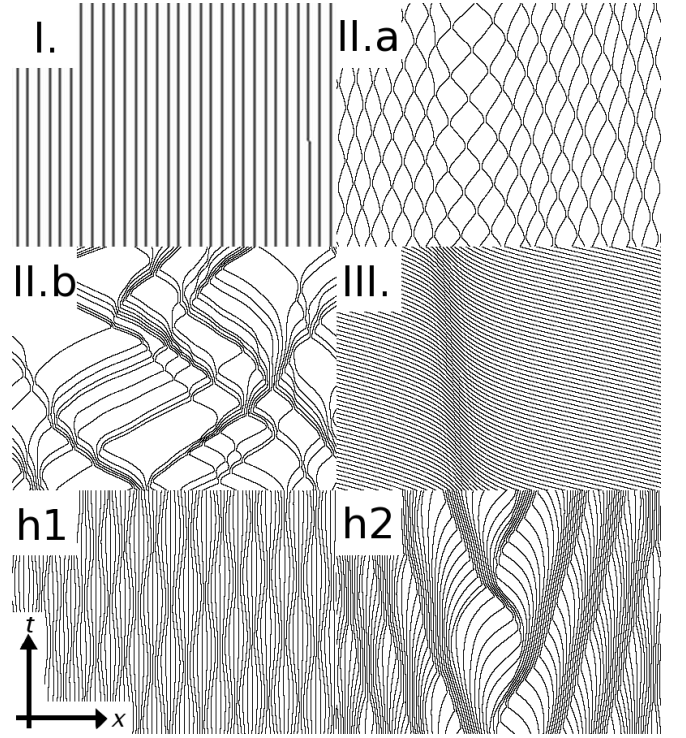


FIG. 1. Space-time diagrams with vertical upward time axis showing I) stationary phase, II.a) synchronized oscillation, II.b) erratic oscillation, III) unidirectional flow. These have a total density of 0.2. Note the left moving dense region in III) representing a jam. h1 and h2 are higher density oscillations corresponding to II.a and II.b (density=0.6).

these patterns are shown in the space-time diagrams of Fig.(1). The key parameter determining the mode of behavior is the viscosity of the water,  $\mu$  in the equations above. It also depends on the total density of boats as described below.

An appropriate choice of order parameter for the transition between stationary and oscillating phases is the root mean square velocity,  $\sqrt{\langle v^2 \rangle}$ . For the transition between oscillating and unidirectionally flowing phases, the order parameter is the average velocity, or flow, of the entire ensemble,  $|\langle v \rangle|$ . These averages are taken over a long time interval ( $\Delta t > 800$ , corresponding to several hundred oscillation periods) beginning after an initial relaxation period. The quantities are then averaged over the ensemble. The initial positions were semi-randomized to break symmetry and the camphor distribution was  $c_0(x) = 0$ .

We will now qualitatively describe the three different types of behavior, enumerated as above, and the transitions between them occurring at the critical viscosities  $\mu_{c1}$  and  $\mu_{c2}$ .

**(I).**In the very high viscosity phase, the system approaches a stable, stationary equilibrium in which the boats are uniformly spaced. This may be related to the phenomenon observed by Soh *et.al.* [17] in which camphor particles arranged themselves into a crystal-like pat-

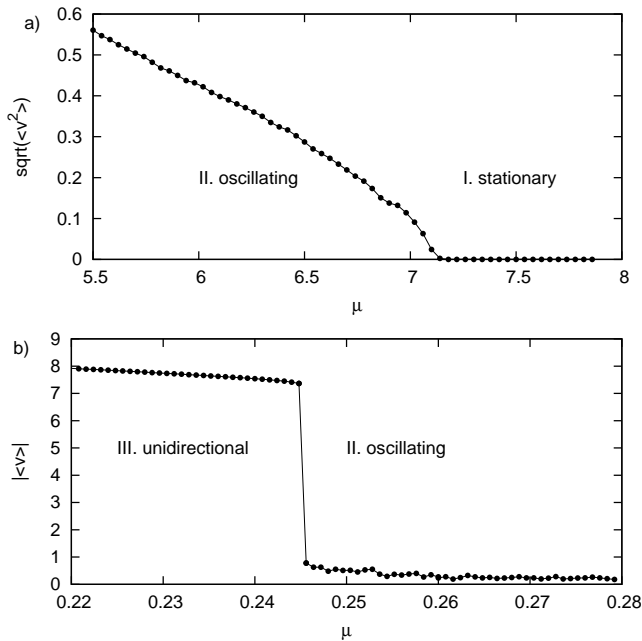


FIG. 2. a)  $\sqrt{\langle v^2 \rangle}$  in the vicinity of  $\mu_{c1}$ . b)  $|\langle v \rangle|$  in the vicinity of  $\mu_{c2}$ . Other parameters are:  $k = 0.072$ ,  $\Gamma = 528$ ,  $\alpha = 7.2$ ,  $r_0 = 0.25$ ,  $R = 75$ ,  $N = 20$

tern. This behavior is similar for all values of density, but in simulation, very low densities may not converge to uniform spacing due to the extremely small interaction between boats at large distances.

**(II).** As the viscosity is decreased beyond  $\mu_{c1}$ , the stationary state becomes unstable and the boats begin to move. This onset of motion can be quantified by an abrupt increase from zero in  $\sqrt{\langle v^2 \rangle}$ . This transition is shown in Fig.2. For total density greater than about 0.15, the boats oscillate and  $|\langle v \rangle|$  remains almost zero. For lower densities,  $|\langle v \rangle|$  depends highly on the initial conditions, but the transition still holds. For densities greater than 0.15, there are two different oscillation patterns depending on viscosity, described here as *a*) and *b*)

*a*) For higher viscosity, the boats oscillate in a very synchronized formation. The qualitative behavior is similar to a set of identical density waves traveling in both directions as shown in Fig.1. To quantify this, we can measure the degree of synchronization between boats using the cross correlation of their velocities. Fig.3 shows the correlation vs. the distance in numbers of boats. If the density is below about 0.4, neighboring boats are anti-synchronized. Higher densities show the strongest anti-synchronization at a distance of several boats. This distance appears to increase with increasing total density.

*b*) For lower viscosity, the oscillations become more irregular and the anti-synchronized behavior vanishes. As seen in Fig.3, the correlation is positive in the vicinity of the boats and drops to almost zero for boats further

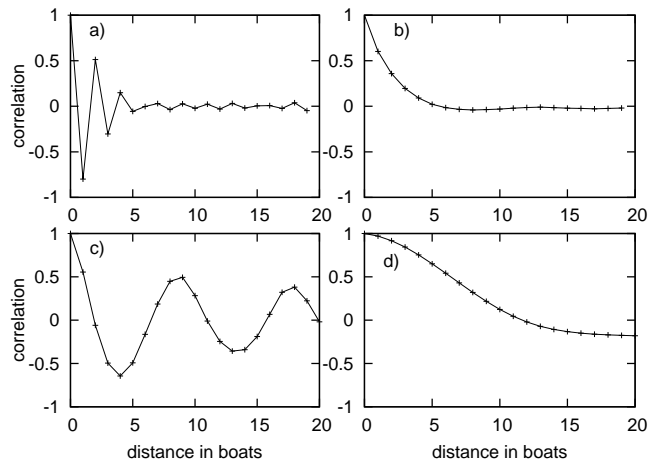


FIG. 3. Cross correlation of velocity vs. distance in boat numbers for a) density=0.26,  $\mu = 0.6$  b) density=0.26,  $\mu = 4.0$  c) density=0.6,  $\mu = 0.12$  d) density=0.6,  $\mu = 0.68$  corresponding to behavior shown in Fig.1 II.a, II.b, h1, h2 respectively

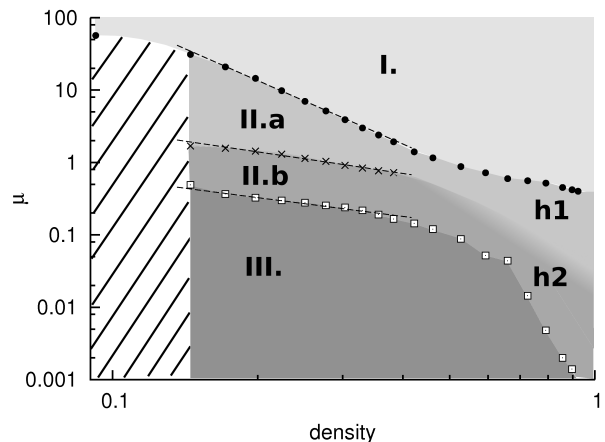


FIG. 4. Phase diagram for the types of behavior. The dashed lines are a power law fit for densities between 0.17 and 0.38, but such a relation is not implied. (same parameters as fig.2)

away. There is no pattern of synchronization and anti-synchronization as seen for type *a*) behavior.

**(IV).** As viscosity is decreased further, the boats oscillate in larger groups and with longer periods between changes in direction. There is a critical viscosity,  $\mu_{c2}$ , below which the boats no longer change direction and the flow becomes unidirectional. The selection of direction is spontaneous and depends on initial conditions. This transition can be seen quantitatively as a discontinuity in the net velocity of the entire system,  $|\langle v \rangle|$ . This is shown in Fig.2.

Fig.4 is a phase diagram illustrating the regions of viscosity and density for each type of collective behavior. A power law fit was made for the density range 0.17 to 0.38, but it is not clear that the data follow such a relation, especially in the case of  $\mu_{c2}$ . Although the critical values

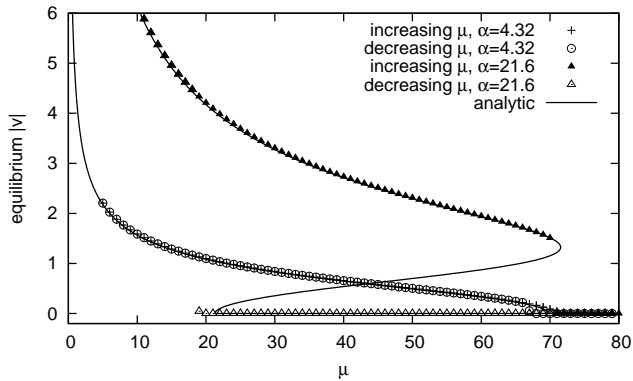


FIG. 5. Equilibrium velocity for  $N = 1$ .

$\mu_{c1}$  and  $\mu_{c2}$  are clearly defined, the change between patterns II.a and II.b is more gradual. The data shown for density between 0.15 and 0.38 correspond to the point at which the average correlation between neighboring boats increases to zero. At higher density the change was too gradual to assign a meaningful transition point, so it is not clearly defined in the diagram. The non-stationary phase for density below about 0.15 depends highly on initial conditions, so the distinction between oscillating and flowing phases is not shown. In contrast, the transition at  $\mu_{c1}$  was consistent even down to the low density limit of a single boat.

The transition at  $\mu_{c1}$  as well as the change from pattern II.a to II.b appear to be independent of the total system size as long as the total density is kept constant. The critical viscosity  $\mu_{c2}$  increases very slightly with increasing system size. This was tested by varying the total route length between  $R = 38$  and  $R = 607$ .

The case of one boat can be treated specially by solving the equations in the moving reference frame of the boat. Assuming that the system has had sufficient time to reach a steady state, the boat will be moving at a constant velocity and the camphor field will be time independent in the moving frame of the boat. The camphor equation can then be solved exactly and the equilibrium viscosity can be computed as a function of velocity. The results show the existence of a critical viscosity above which the zero-velocity state is stable, corresponding to the transition between the stationary and oscillating phases. The type of bifurcation at this point depends on various system parameters. For example, Fig.5 shows two different camphor supply rates ( $\alpha$  in eq.6). The bifurcation for the lower rate is supercritical, while that for the higher rate is subcritical. The resulting hysteresis was also observed in a one-boat simulation as shown in the figure. Although this analysis appears to work well for the case of one boat, it does not apply directly to systems containing more boats due to the constant velocity, steady state assumption. Thus it can not explain the oscillatory behavior or the  $\mu_{c2}$  transition.

In summary, we have simulated a one dimensional system of symmetric camphor boats and observed three different phases of collective motion. The transitions between these phases can be quantified by abrupt changes in the average flow,  $|\langle v \rangle|$ , and the root mean square velocity,  $\sqrt{\langle v^2 \rangle}$  of all the boats in the system. We have described some of the qualitative features of the collective motion and presented the results of numerical simulations. In future work, we hope to test these results through experiment. One significant challenge will be reproducing the range of parameters required to observe the different types of behavior.

This work is supported by Grants-in-Aid for Scientific Research(No.22540391) to H.N. and for Young Scientist(B)(No.23740299) to N.J.S. from the Ministry of Education, Science and Culture of Japan and the Global COE Program Formation and Development of Mathematical Sciences Based on Modeling and Analysis.

- 
- [1] I. D. Couzin and J. Krause, *Advances in the Study of Behavior*, **32**, 1 (2003), ISSN 0065-3454.
  - [2] J. Buhl, D. J. T. Sumpter, I. D. Couzin, J. J. Hale, E. Despland, E. R. Miller, and S. J. Simpson, *Science*, **312**, 1402 (2006).
  - [3] T. Vicsek and A. Zafiris, *ArXiv e-prints* (2010), arXiv:1010.5017 [cond-mat.stat-mech].
  - [4] D. L. Blair, T. Neicu, and A. Kudrolli, *Phys. Rev. E*, **67**, 031303 (2003).
  - [5] J. Deseigne, O. Dauchot, and H. Chaté, *Phys. Rev. Lett.*, **105**, 098001 (2010).
  - [6] T. Vicsek, A. Czirók, E. Ben-Jacob, I. Cohen, and O. Shochet, *Phys. Rev. Lett.*, **75**, 1226 (1995).
  - [7] A. Czirók, A.-L. Barabási, and T. Vicsek, *Phys. Rev. Lett.*, **82**, 209 (1999).
  - [8] H. Levine, W.-J. Rappel, and I. Cohen, *Phys. Rev. E*, **63**, 017101 (2000).
  - [9] G. Grégoire and H. Chaté, *Phys. Rev. Lett.*, **92**, 025702 (2004).
  - [10] A. Czirók, H. E. Stanley, and T. Vicsek, *Journal of Physics A: Mathematical and General*, **30**, 1375 (1997).
  - [11] E. Bertin, M. Droz, and G. Grégoire, *Phys. Rev. E*, **74**, 022101 (2006).
  - [12] M. R. D'Orsogna, Y. L. Chuang, A. L. Bertozzi, and L. S. Chayes, *Phys. Rev. Lett.*, **96**, 104302 (2006).
  - [13] A. Baskaran and M. C. Marchetti, *Phys. Rev. Lett.*, **101**, 268101 (2008).
  - [14] S. Mishra, A. Baskaran, and M. C. Marchetti, *Phys. Rev. E*, **81**, 061916 (2010).
  - [15] S. Nakata, Y. Doi, and H. Kitahata, *The Journal of Physical Chemistry B*, **109**, 1798 (2005).
  - [16] N. J. Suematsu, S. Nakata, A. Awazu, and H. Nishimori, *Phys. Rev. E*, **81**, 056210 (2010).
  - [17] S. Soh, K. J. M. Bishop, and B. A. Grzybowski, *The Journal of Physical Chemistry B*, **112**, 10848 (2008).
  - [18] N. J. Suematsu, Y. Ikura, M. Nagayama, H. Kitahata, N. Kawagishi, M. Murakami, and S. Nakata, *The Journal of Physical Chemistry C*, **114**, 9876 (2010).